Hindawi
Journal of Nanomaterials
Volume 2022, Article ID 8005644, 14 pages
https://doi.org/10.1155/2022/8005644

Research Article

Application on the Luminescence Characteristics of Nanoaluminate Rare Earth Long-Lasting Luminescent Composite Materials in the Field of Ethnic Clothing

Jiaxi Huang and Zhimin Gao

College of Fine Arts and Design, Huaihua University, Huaihua, 418000 Hunan, China

Correspondence should be addressed to Zhimin Gao; gzm@hhtc.edu.cn

Received 20 January 2022; Revised 25 February 2022; Accepted 7 March 2022; Published 30 March 2022

Academic Editor: Palanivel Velmurugan

In the changing process of garment development, nanoaluminate rare earth material has unique advantages as a new garment material, such as easier preservation and brighter color, changing the visual beauty of traditional clothing. In order to in-depth study the role of nanoaluminate rare earth long afterglow luminescent composite materials applied to ethnic costumes, this article uses material preparation methods, numerical analysis adjustment methods, and equipment parameter introduction methods to analyze nanoaluminate rare earths and simplify them and create a luminous composite material that can be used in the field of ethnic minority clothing. To study the luminescence characteristics of the composite material, CXHP samples with different doping concentrations of Cr ions were irradiated with an ultraviolet lamp with a center wavelength of 225 nm for 4.5 minutes, and after 12 minutes attenuation, the afterglow emission spectrum was studied. The results show that the sample has near-infrared afterglow emission ranging from 645 nm to 740 nm, and the two emission peaks are located at 680 nm and 700 nm, respectively. The performance of its application on clothing was studied again. The water consumption in the experiment was 1500 ml, and the grams of composite material added for the three times were 0.6 g, 1.2 g, and 1.8 g, respectively. The hanging dyeing method was adopted during the experiment. Through experiments, it can be obtained that when the composite material is 1.8 grams, the visual effect is more similar to the hue, brightness, purity, and other aspects of the clothing. This way, when combined with the composite material for secondary design, a better visual effect will be achieved. From the practical application level, it has been verified that composite materials can be used in ethnic costumes.

1. Introduction

In recent years, with the continuous advancement of various sciences and technology of nanomaterials, the research of rare earth luminescent materials has been further developed. Within the nanometer standard size, due to special effects such as surface reaction, quantum measurement effect, small size effect, and macroscopic quantum tunneling effect, nanomaterials exhibit many mechanical, electrical, magnetic, and optical properties that are distinct from general materials. Rare earth-doped nanoluminescent materials have excellent optical properties such as good light stability, large Stokes/anti-Stokes shift, long fluorescence lifetime, and narrow spectral line width. They are used in ultrasonic inspection, detection, treatment, luminescence display, photovoltaic devices, and other fields show broad application prospects and have become a hot research topic in recent years.

As the carrier of the traditional culture of ethnic minorities, ethnic clothing is not only an important mark of each ethnic group but also an indispensable part of the cultural heritage of ethnic minorities. It is the precious wealth of the entire Chinese nation. Inheriting and protecting the traditional culture of ethnic minority clothing is nowadays new topics of general concern to society. However, with the influence of various factors such as economic globalization and social modernization, the ethnic costume culture that has sunk for thousands of years has almost disappeared, and some have even disappeared. The protection situation is very

strict. Although there are already some protection methods and research methods, they are far from enough, and modern chemical methods are needed. It is of irreplaceable significance to use nanoaluminate rare earth long afterglow luminescent composite materials to preserve ethnic costumes and to study whether their luminous characteristics can reproduce the gorgeousness of ethnic costumes.

Many scholars have been doing research on ethnic minority clothing for a long time, but in recent years, more and more scholars have begun to study the luminescence properties of composite materials on clothing. In 2016, Kaewkhao et al. observed the highest emission intensity in the development glass prepared under the condition of 0.4 mol% Dy_2O_3. From the perspective of X-ray-induced optical luminescence, the emission spectrum is the same as the emission spectrum measured by PL, but the intensity observed on the glass quenched with 0.45 mol% Dy_2O_3 is the highest. Finally, the overall scintillation efficiency of the developed nanocomposite glass was determined to be 27% of that of commercially available BGO crystals. However, their research is not rigorous [1]. In 2017, the purpose of Hernández was to study the luminescence properties of lanthanum aluminate powders prepared by improved Pechini (MP) method. The samples were prepared with different Eu^{3+} concentrations and calcined at 1600°C. The luminescence characteristics are analyzed by photoluminescence (PL) and thermoluminescence phenomena. Studies have shown that polycrystalline $LaAlO_3 : Eu^{3+}$ powder calcined at 1600°C has interesting luminescence properties. But this research is radioactive and harmful to humans [2]. In 2018, Oleshko et al. studied the emission spectra and dynamics of Sn- and Fe-doped Ca_2O_3 crystals excited by nanosecond electron beams. Compare with data obtained using electron beam current pulses of sub-nanosecond duration. The results show that as the duration of the beam pulse increases, it is produced by cathodoluminescence in the range of 300-450 nm. However, there are errors in the experimental process [3]. In 2017, Bezkrovnaya et al. studied the spectral and luminescence properties of three laser dyes in the 600-700 nm spectral range. These dyes were incorporated into a xerogel matrix preliminarily calcined at 700 C. Compared with methanol, this effect is manifested in reducing nonradiation losses and increasing the quantum yield of dye luminescence in the calcined xerogel in this state. Unfortunately, there is no research on its application [4]. In 2021, Kyselova and Shandrenko explained how to find harmony in modern clothing design projects. Research methods include analytical applications in the field of fashion, as well as methods of source, aesthetics, and structural composition analysis. Conclusion: design forms and expressions are mainly due to changes in social needs, value systems, and psychological norms. Among them, seeking harmony is also very important-external and internal. However, the research did not involve composite luminescent materials [5]. In 2016, Krause et al. constructed a multivariate model to examine the extent to which sociodemographic, interpersonal, and behavioral factors explain the instability of minority housing. A composite optical instrument was used to collect data. The research found that housing instability may originate from early life experiences and proposed an intervention point to prevent the housing instability of sexual minority males. But the basic research approach is wrong [6]. In 2020, in order to use commercial sulfur-based cathodes to obtain sufficient capacity and long-term cycle performance, Ghosh et al. introduced ultrathin lithium aluminate nanosheets as a polysulfide fixing agent with excellent lithium ion conductivity. At the high current speed of 3 C, the capacity decay rate per cycle is extremely low, only 0.02%. This work demonstrates a promising strategy to directly utilize commercial sulfur powder in actual lithium-sulfur batteries. However, the research purpose is not pure enough [7].

The innovations of this paper are as follows: (1) The effects of solvothermal conditions and the organic additive sodium citrate on the crystal phase, morphology, size, crystallinity, etc. of the product are systematically studied. (2) The temperature-varying fluorescence test shows that the nanocrystals are superior. The conversion luminescence characteristics can be well matched within the temperature range of 10-623, and the sensitivity is equivalent to the reported rare-earth-doped upconversion fluorescence thermometer. (3) We have found a universally adjustable rare earth upconversion nanomaterial luminescence performance. The method provides a theoretical basis for future material selection. Through the above work, it is ensured that the composite material or product proposed in this paper has good performance and can be used in ethnic minority clothing. (4) This paper uses energy transfer technology and thermal decomposition method to decompose the luminescent components in the nanoaluminate rare earth long-acting luminescent composites. Finally, it is concluded that how the nanoaluminate materials promote the effect of clothing luminescence.

2. Method Based on the Luminescent Properties of Nanoaluminate Rare Earth Composite Materials in Ethnic Costumes

2.1. Introduction to Ethnic Costumes. National costumes refer to the costumes of ancient costumes that still uphold and maintain the inherent characteristics of each ethnic group over time. Specifically, it refers to materials, patterns, luster, patterns, and production techniques that are less affected by other ethnic cultures. The influence of this country still retains more of the national style and characteristics, clothing that can represent and reflect the characteristics of the national history and culture [8]. Our country is a multi-ethnic country with 56 ethnic groups. In the long historical development, each ethnic group has formed a totem that can reflect the traditional culture, religious beliefs, living habits, ethnic consciousness, geographical environment, artistic tradition, aesthetic concepts, and totems of their own ethnic groups. They worship the unique costumes. For example, the Yi people admire martial arts. They believe that the tiger is a symbol of bravery and sturdiness. Therefore, the tiger totem is the most common totem pattern in Yi costumes; Yi women often embroider small figures on

the trousers, reflecting the Yi people's preference for many children and grandchildren. The Miao people regard the butterfly as the founder of the world, and respectfully call it the "butterfly mother." In order to highlight the Miao people's admiration for the butterfly mother, the Miao people use the butterfly as their totem; the Miao people believe that humans evolved from dragons, Nuwa. The prototype is the body of the human head dragon, respecting the dragon and offering sacrifice to the dragon is equivalent to respecting the ancestor and offering sacrifice to the ancestor. The Miao people naturally regard the dragon as their own totem [9]. This article has found some national costumes, as shown in Figure 1 [10].

It can be seen from Figure 1 that each ethnic group has its own totem worship, which is directly reflected in their clothing. Therefore, the clothing of each ethnic group contains its unique totem, pattern style, and other important element structures, and the element structure is the main basis for the study of national costumes in this article [11].

2.2. Nanoaluminate Rare Earth and Its Luminescence Characteristics. Solid luminescence dynamics introduced the movement mechanism and forms of glow ion center excited state. Contents include the center of the ion transition, electron phonon interaction, and interaction between ions influence on luminescence process; this paper use of luminous dynamic ion elements contained in the dress material is analyzed, and examples to illustrate.

(1) Rare earth elements

Rare earth elements are a collective term of 17 elements in total from 15 lanthanides from 57 to 71 in the periodic table. Rare earth elements have similar chemical properties, close ionic radius, and symbiosis in nature [12]. Because rare earths coexist in nature, it was difficult to study rare earths in the past where the separation technology was not developed. Therefore, it was mistaken that the content of rare earth elements was scarce, so it was named rare earth. It has been found that rare earth elements are not scarce. For example, cerium (Ce) is ranked 25th in the earth's crust in abundance, which is higher than lead; the lowest rare earth element lutetium (Lu) is also more abundant than common metals. Gold is nearly two hundred times higher [13].

(2) Nanomaterials

Nanomaterials, also known as ultrafine particle materials, are mainly composed of two parts: nanocrystalline grains and grain interfaces. The size of the nanoparticle is very close to the size of the atom, but it is neither a microscopic system in the general sense nor a typical macroscopic system, but a mesoscopic system. Because of its very small particle size, it has many novel characteristics, which are different from the microscopic properties of the constituent material units-atoms and molecules, and also different from the macroscopic properties of the material materials [14].

(3) Aluminate

Aluminate-based luminescent materials have become a research hotspot in the field of luminescent materials in recent years due to their very stable physical and chemical properties, simple synthesis process, relatively low synthesis temperature, and excellent luminescence performance [15]. Upconversion luminescent materials usually consist of a matrix and an activator, and some materials also contain a sensitizer. Rare earth ions have a rich energy level structure and are currently used as activators for up-conversion materials [16]. According to the matrix components, currently commonly used upconversion luminescent materials can be divided into fluorides, oxides, sulfides, and composite oxides. From the perspective of practical application, the matrix material must have good chemical stability, thermal stability, and good corrosion resistance.

Aluminates in oxides are often used as luminescent matrix materials due to their excellent chemical and thermal stability. For example, they are often used as long afterglow luminescent matrix. As a member of aluminate family, dodecalcium heptaaluminate is often used as rare earth, with low cost and the lowest synthesis temperature in this system. Due to its special nanocage structure, especially the weakly bound anions in the cage, it has a wide application prospect in the fields of electronic compounds and catalysis. At the same time, the weakly bound anions in the cage can also be used to regulate the luminescence characteristics of rare earth luminescent ions. As previously used in this group, the anion in the cage is replaced with easily conductive, which improves the cathodoluminescence of C12A7: CE and obtains low-voltage excited field emission display phosphors. In addition, by replacing the anion in the cage in C12A7 : EU, the modulation of radiation transition probability and nonradiation transition probability is realized, so as to adjust its luminescence characteristics. Figure 2 is a schematic diagram of the crystal structure of [17].

It can be seen from Figure 2 that studies have shown that the inherent disorder makes $CaGdAlO_4$ a better luminescent host material [18]. Chemical precipitation method is also one of the methods of separation and purification. It makes the target component (ion) in the solution selectively precipitate out in the form of insoluble compounds by virtue of the role of precipitant. In the study of luminescence dynamics, the experimental light path is shown in Figure 3.

It can be seen from Figure 3 that through the construction of the experimental optical path, we can study the preparation method of rare earth luminescent nanomaterials, and the thermal decomposition method is selected in this article. Thermal decomposition is heating metal oxides, iodides, carbonyl compounds, and so on to decompose pure metal, generally applicable to silver, mercury, and other inactive metal elemental extraction. The synthesis of nanoparticles by thermal decomposition is the most commonly used method among many wet chemical synthesis methods, usually under anhydrous and oxygen-free conditions. The nanoparticles obtained by the method have high crystallinity, good dispersibility, and controllable morphology and crystal phase. First, the metal organic compound (usually

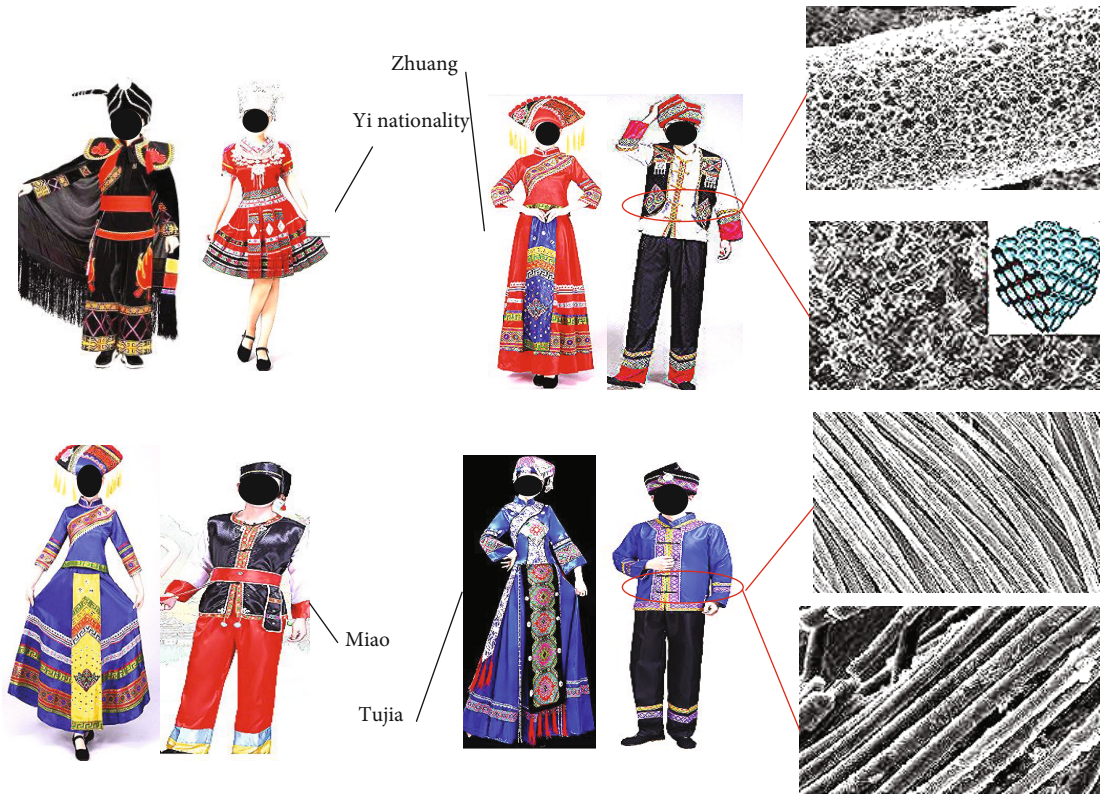

Figure 1: National costumes of the Yi, Miao, Zhuang, and Tujia nationalities.

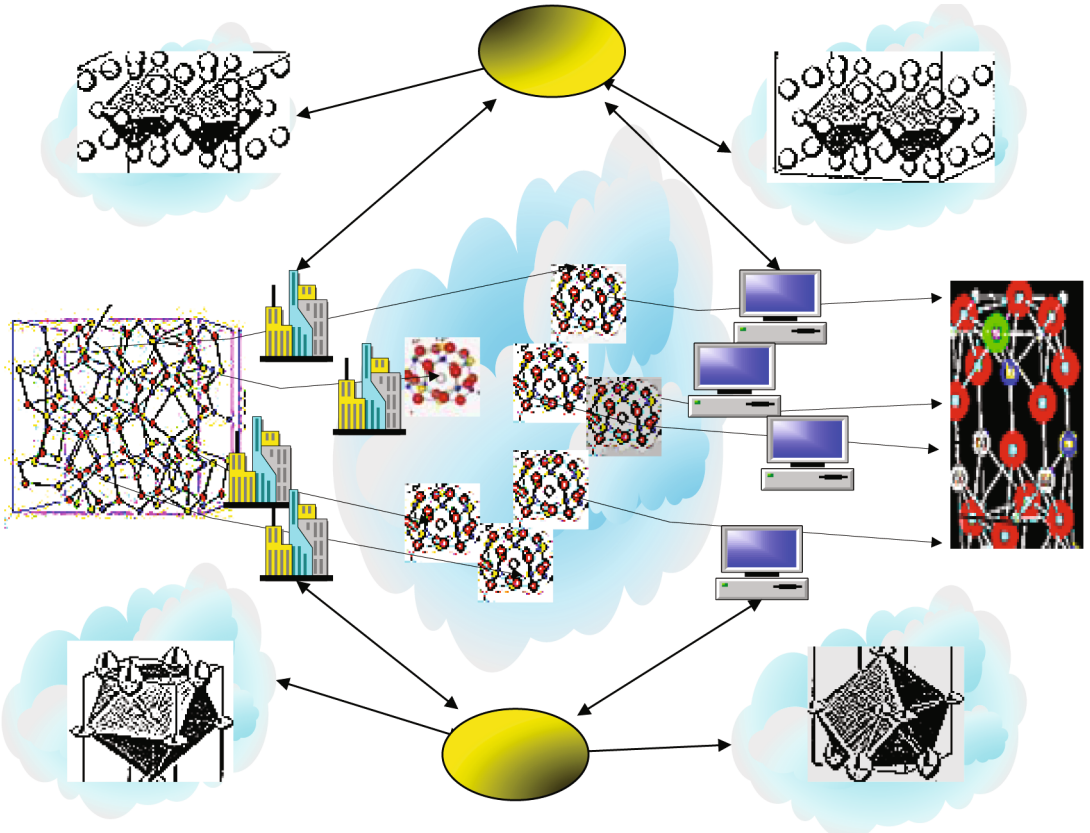

Figure 2: Schematic diagram of crystal structure.

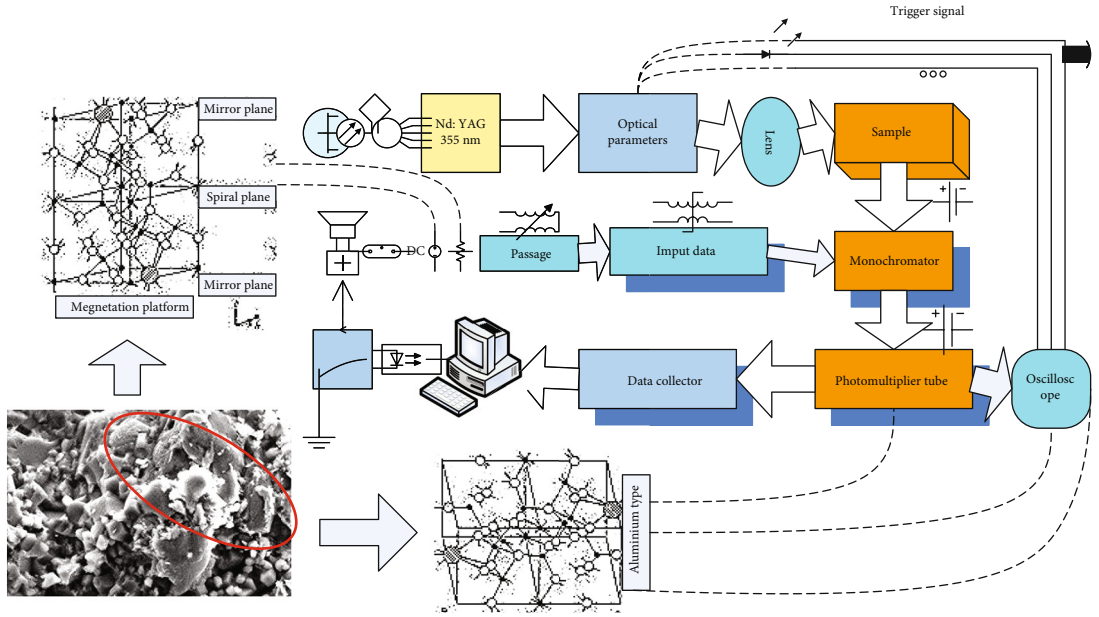

Figure 3: Schematic diagram of luminescence dynamics test device.

metal trifluoroacetate) is used as a precursor, and it is added to a high-boiling organic solvent with coordination properties, and then, the temperature is increased; the precursor decomposes and crystallizes into a nucleation reaction. The specific process is shown in Figure 4 [19].

It can be seen from Figure 4 that octadecene (ODE) is generally used as a solvent during the thermal decomposition reaction because of its higher boiling point. Oleic acid (OA), oleylamine (OM), and trioctyl phosphine oxide (TOPO) have groups that can coordinate with metal ions and are often used as surfactants, and all three structures contain long hydrocarbon chains, which can be effective in preventing agglomeration of nanoparticles [20]. During the reaction process, by adjusting the reaction temperature, reaction time, surfactant type, precursor concentration, etc., rare earth upconversion luminescent nanoparticles with good crystallinity, monodisperse, and controllable morphology and size can be obtained [21].

(4) Algorithms involved

Diffraction technology is a method of incident high-energy electron beam with respect to the atomic plane of the crystal sample at a specific angle, resulting in strong elastic scattered waves, mutual interference, and characteristic electron diffraction patterns related to the crystal structure. The crystal structure can be analyzed by using this mode. We use an integrating sphere with a combined fluorescence spectrometer to test the absorptivity and quantum efficiency of the material. When testing, we set the slit, excitation, and emission wavelengths, i_x, i_y, and i_z as required and calculate the absorption rate through the following formula [22]:

$$\mathrm{x} = \frac{i_y - i_z}{i_y} + \sqrt{u_a + u_b} + \frac{1}{2}. \tag{1}$$

Among them, x is the total score, test f_y and f_f as required, and calculate the quantum efficiency according to the following formula [23]:

$$\varpi_1 = \frac{f_f - (1-x) * f_y}{i_x * x}. \tag{2}$$

When $a \geq 0.05$, the XRD diffraction peak position appears to shift significantly. This is because according to the Bragg equation,

$$2\mathrm{w}\cos\mu = \mathrm{o}\beta \pm \coprod_{\eta}^{\nabla} \xleftarrow{\gamma} \Psi. \tag{3}$$

Among them, w represents the interplanar spacing; this is because according to the calculation formula of the concentration quenching critical distance e_f proposed by B:

$$\mathrm{e}_f = 2\left(\frac{3m}{4\mu a_z o}\right)^{1/3} + \sum \mathfrak{RF}. \tag{4}$$

Among them, m represents the unit cell volume, where the absorption rate is calculated by the following formula:

$$\mathrm{x} = \frac{i_y - i_z}{i_y^z} * \left[\frac{1}{2} \oplus \prod_y z\right]. \tag{5}$$

Among them, x represents the absorption rate of the phosphor; i_y represents the scattering on the surface of the integrating sphere when the phosphor and the

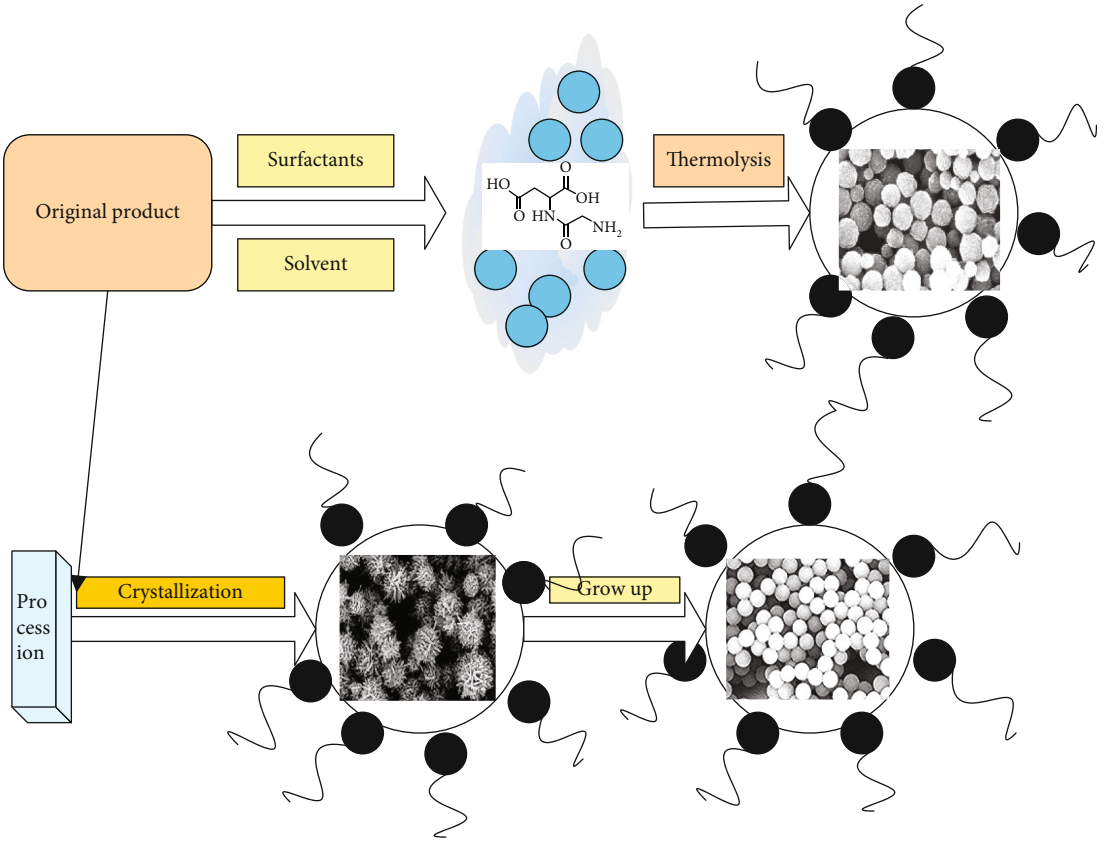

Figure 4: Schematic diagram of synthesis of nanoparticles by thermal decomposition reaction.

excitation light are not on the same optical path; the quantum efficiency is calculated by the following formula:

$$\vartheta_e = \frac{f_f - (1-x) * f_y}{i_v * x} + \frac{1}{3}. \tag{6}$$

ϑ_e represents the quantum efficiency; f_y represents the emission intensity detected when the phosphor and the excitation light are not on the same optical path; using the Arrhenius formula:

$$u_s = \frac{u_p}{1 + zuzi(-f_x/gs)}. \tag{7}$$

Among them, u_s represents the luminous intensity of the phosphor at a certain temperature; after the above formula is mathematically processed, the following another expression form can be obtained:

$$\text{out}\left(\frac{u_p}{u_s} - 1\right) = -\frac{z}{gs} * f_x. \tag{8}$$

The converted Arrhenius formula can be regarded as a linear function of $\text{out}((u_p/u_s) - 1)$ versus $-z/gs$, the fluorescence decay curve of the phosphor and use the first decay function with origin software.

$$u_s = u_p uzi(-s/v) + \oiint_{wu}\left(\frac{xe}{2}\right). \tag{9}$$

According to the energy transfer efficiency formula,

$$\sigma_s = 1 - \frac{\varsigma_p}{\theta_t} + \frac{\infty}{\psi} * \left[\sum_y^x l + \sum_z l\right]. \tag{10}$$

Among them, σ_s represents the energy transfer efficiency; according to Dexter's energy transfer equation for multipole action, we know

$$\frac{\mu_p}{\mu_t} \in z^{o/3}_{sy^{3+}+fv^{3+}} + z_c. \tag{11}$$

Among them, μ_p represents the quantum efficiency of a single-doped sy^{3+} sample; the value of μ_p/μ_t is similar to u_p/u_t, so

$$\frac{u_p}{u_t} \in z^{o/3}_{sy^{3+}+fv^{3+}} + u_c + u_b. \tag{12}$$

The ratio of the fluorescence intensity of the upper and lower energy levels of the thermal coupling energy level of Er^{3+} is in accordance with the following relationship:

$$e = \frac{u_{522}}{u_{550}} = e_p uzi\left(-\frac{\nabla f}{-g_y s}\right). \tag{13}$$

Among them, u_{522} and u_{550} are the integrated intensity of green light emission at 522 nm and 550 nm, respectively, e_p is a proportional constant independent of temperature, ∇f is the energy level difference of the thermal coupling energy level of Er^{3+}, and s is the thermodynamic temperature. Further, according to formula (13), the linear relationship can be as follows:

$$uoe = \text{out}\frac{u_{522}}{u_{550}} = -\frac{\nabla f}{g_y s}\frac{1}{s} + z. \tag{14}$$

In the upconversion fluorescence thermometer based on the fluorescence intensity ratio of the thermal coupling energy level pair of Er^{3+}, an important parameter to be investigated is the relative sensitivity of the temperature measurement [24]. It can be expressed as

$$t_e = \frac{1}{e}\frac{\text{we}}{ws} = \frac{\nabla f}{g_y s^2}. \tag{15}$$

According to the Boltzmann distribution, the population of particles on the energy level is related to the energy of the energy level, the surrounding temperature and the degeneracy of the energy level. The specific relationship is

$$\text{o}_u = h_u uzi\left(-\frac{f_u}{g_y s}\right) - \frac{f_k}{m_b t}. \tag{16}$$

Among them, h_u represents the degeneracy of the energy level, f_u is the energy of the energy level, g_y is Boltzmann's constant, and s is the Kelvin temperature. When the energy level interval is Δf, the ratio of the number of particles in two adjacent energy levels is

$$\frac{\text{o}_2}{o_1} = \frac{h_2}{h_1} uzi\left(-\frac{\nabla f}{g_y s}\right). \tag{17}$$

Among them, o_2 represents the number of particles at a high energy level, o_1 represents the number of particles at a low energy level, h_1 and h_2, respectively, represent the degeneracy of these two energy levels, and the relationship between the fluorescence intensity and the number of particles is also known:

$$u_u = \varepsilon o_u \omega_{\text{up}} gz\rho_{\text{up}} + \pi 0_{\text{up}} y\lambda\rho_{\text{up}}, \tag{18}$$

where u_u is the upconverted fluorescence intensity and ε is a set factor related to the structural environment; therefore,

$$\frac{u_2}{u_1} = \frac{\partial_{20}\omega_{20} o_2}{\partial_{10}\omega_{10} o_1} = \frac{\partial_{20} h_2 \omega_{20}}{\partial_{20} h_1 \omega_{10}} uzi\left(-\frac{\nabla f}{g_y s}\right). \tag{19}$$

An important parameter to be studied in the conversion of the rate of catalytic reactions into fluorescent thermometers based on thermal coupling is the relative sensitivity of temperature measurements. For Er^{3+} ion, it can be expressed as

$$e = \frac{u_{522}}{u_{558}} = \frac{o\left({}^2 g_{10/2}\right)}{o\left({}^2 t_{3/2}\right)} = \frac{h_g \partial_g \omega_g}{h_t \partial_t \omega_t} uzi\left(-\frac{\nabla f}{g_y s}\right) = zuzi\left(-\frac{\nabla f}{g_y t}\right). \tag{20}$$

Among them, e is a constant; in other words, for the same sample, its ratio can be used to characterize the temperature of the sample [25].

2.3. Long Afterglow Luminescent Materials. "Luminescence" is a kind of nonequilibrium radiation, which means that under the excitation of some external conditions (light mapping, external electric field or electron beam bombardment, etc.), the object absorbs external energy, and the system deviates from the original equilibrium state. Energy transfer refers to the process of energy transfer from high-temperature region to low-temperature region. The mechanisms of energy transfer include conduction, convection, and radiation. In the process of restoring to the equilibrium state, the object emits excess energy in the form of light in addition to thermal radiation. The emission process has a certain duration, that is, after the external excitation stops, the brightness will not disappear immediately, but gradually weaken. Afterglow is the phenomenon that light can be continuously emitted when the external action stops. Long afterglow is a special phenomenon that materials with energy storage function absorb the energy radiated by external light and store it. After the excitation stops, they slowly release the stored energy by emitting light under appropriate conditions.

A long afterglow luminescent material is a special photoluminescent material, which can absorb the energy irradiated by external light such as visible light or ultraviolet light and store it. After the projection stops, under certain conditions, the stored energy will slowly emit light in the form of light. Long afterglow luminescent materials have been widely used in architectural decoration, information display, and safety instructions and are now gradually expanding to application fields such as information anti-counterfeiting, biological detection, and optical imaging. In the application of biomedical imaging, long afterglow luminescent materials have special advantages: ultralong afterglow lifetime, which can delay detection and imaging. Other energy transfer methods include energy transfer on the same potential energy surface, such as rotation translation, rotation, vibration, vibration translation, and vibration rotation, as well as energy transfer involving the change of electronic state of species, such as electron translation, electron vibration, and electron. Long afterglow materials can be excited in vitro, thereby effectively avoiding tissue auto fluorescence and reducing damage to cell tissues. And the biological transmission window is 600-900 nm; the light

in this wavelength range is the least absorbed by water, which accounts for the largest proportion of the human body; and its luminescence mechanism is shown in Figure 5. Working in the near-infrared region can increase the transmittance of the deep tissue of the detection light. Therefore, the application of near-infrared long afterglow luminescent materials in the optical imaging of living organisms can effectively avoid interference, achieve high signal-to-noise ratio, and obtain better imaging results. The action of a catalyst to change the rate of a chemical reaction is called catalysis, and it is essentially a chemical effect. Chemical reactions take place in the presence of a catalyst. This reaction is called catalytic reaction. Catalysis is an important phenomenon that exists in nature and covers almost the entire field of chemical reactions. Therefore, near-infrared long afterglow materials have outstanding advantages in bioimaging. They are the most potential bioluminescent markers and have become a research hotspot.

It can be seen from Figure 5 that, so far, the research on visible light long-lasting luminescent materials based on rare earth ion- (Eu^{2+}-) doped aluminate and silicate systems has achieved rapid development. When a catalyst is added, the aluminate and silicates react slowly. According to the type of matrix, long-lasting luminescent materials are mainly divided into several major systems; this article focuses on the aluminate system.

Since et al. discovered that $SrAl_2O_4 : Eu^{2+}$ has long afterglow characteristics in 1968; the long afterglow luminescent material of the aluminate system has been highly concerned by researchers. In 1996, after Ma et al. synthesized the $SrAl_2O_4 : Eu^{2+}, Dy^{3+}$ long afterglow material with excellent performance by codoping with europium ion (Eu^{2+}) and dysprosium ion (Dy^{3+}), blue long afterglow materials and red long afterglow materials were also developed one after another. It can be seen that the aluminate long afterglow material mainly uses Eu^{2+} ions as the activator, alkaline earth metal aluminates as the matrix, and rare earth ions such as Dy^{3+} and Nd^{3+} as auxiliary activators. The role of catalysts in chemical reactions is shown. In a catalytic reaction, the catalyst reacts with the reactants, changing the reaction pathway and thus reducing the activation energy of the reaction. Aluminate system materials have outstanding advantages such as long afterglow time, good light stability, better chemical stability, simple production process, and environmental protection, which makes researchers attach great importance to their research and become the second generation of main long-lasting materials. However, the aluminate system materials also have the disadvantage of being unstable in water, and their luminous color is boring, concentrated in the blue-green color of 420-500 nm, which limits its application to a certain extent.

Now, the relevant research is mainly carried out from two aspects: one is to adjust the element composition ratio and other methods to find new aluminate matrix materials; the other is to dope appropriate luminescent centers to expand the luminous color range of aluminate materials. The commonly used materials of aluminate system can be seen in Table 1.

3. Experiments and Conclusions Based on the Design and Realization Method of the Luminescent Properties of Nanoaluminate Rare Earth Composite Materials in the Application of Ethnic Minority Clothing

3.1. Selection of Experimental Reagents and Equipment. The name, molecular formula, concentration, and detailed information of the manufacturer of the main samples used in the experiment are shown in Table 2.

The main equipment used in the experiment is shown in Table 3.

3.2. Sample Synthesis Method and Steps. All the samples in this paper are synthesized by a simple high-temperature solid-phase method. The flow chart of the synthesis steps of the high-temperature solid-phase method is shown in Figure 6.

It can be seen from Figure 6 that the raw materials are weighed according to the stoichiometric ratio and placed in an agate mortar for uniform grinding for 20 minutes. The obtained mixture was transferred to a corundum crucible and placed in a box-type resistance furnace for pre-sintering at 850°C for 4.5 hours. The obtained prefired product was uniformly ground for 12 minutes and then transferred to a corundum crucible again and placed in a box-type resistance furnace for calcination at 1100°C for 1.5 hours. The obtained product is ground into powder to obtain the product, which is bagged for later use. Part of the samples needs to be synthesized in a reducing atmosphere, just place the corundum crucible containing the sample in a large corundum crucible filled with reduced carbon particles to form a simple reduction device.

3.3. Preparation Conditions. We use the high-temperature thermal decomposition method to change the reaction conditions in the experiment, such as the total amount of reactants, the type and amount of alkali, the reaction time, and the reaction temperature, to achieve a series of super grain sizes ranging from 2.2 to 10.1 nm. For precise control of small nanocrystals, the specific preparation conditions are shown in Table 4.

3.4. Luminous Performance Research. For the convenience, we denoted $Zn_3Al_2Ge_3O_{12}$ as CXHP. We weigh each initial raw material accurately according to the stoichiometric ratio. The weighed raw materials are put into an agate mortar, mixed and fully ground for about 1.2 hours, and then pressed by a powder tablet machine at a pressure of 10 MPa for about 12 minutes, and pressed into a diameter of 16 mm and a height of about 2.1 mm. Then, the disc-shaped sample is placed on the corundum crucible, placed in a box-type high-temperature sintering furnace, and sintered in the air. The sintering temperature is set to 1250°C, the temperature is kept for 11 hours, and the heating rate is 4.9°C/min. Finally, wait for it to cool to room temperature and take it out to get the desired sample.

The Cr^{3+} ion is a typical transition metal ion with a 3d electronic configuration, because its 3d electrons are directly exposed to the outside, lacking an effective barrier for outer

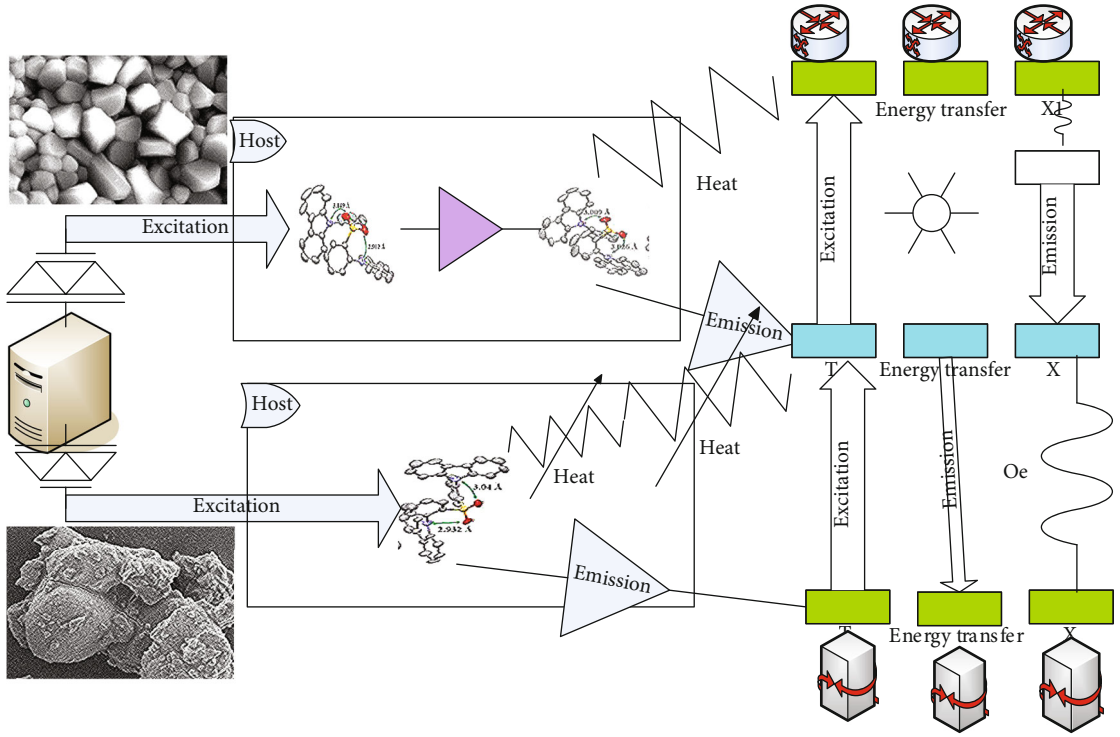

Figure 5: Mechanism of phosphors with sensitizer.

Table 1: Aluminate system Longhui material.

Matrix	Activator	Emit peak (nm)	Yu Hui time
$SrAL_2O_4$	Eu^{2+}, Dy^{3+}	510	>30 h
$CaAL_2O_4$	Eu^{2+}, Nd^{3+}	440	>16 h
$BaAL_2O_4$	Eu^{2+}, Dy^{3+}	490	>2 h
$SrAL_2O_4$	$Cu^{3+} \longrightarrow Zn^{2+}$	510	>5 h
$Sr_4AL_{14}O_{25}$	Eu^{2+}, Dy^{3+}	480	>20 h

electrons, and it is obviously affected by the crystal field environment. Figure 7 is the energy level splitting T-S diagram in the octahedral crystal field, which reflects the relationship between the crystal field splitting energy f of the transition metal ion energy level and the crystal field parameters.

It can be seen from Figure 7 that it reflects the relationship between the crystal field splitting energy f of the transition metal ion energy level and the crystal field parameters. It represents the strength of the crystal field and is related to the average distance between the metal ion and the surrounding lattice ions. Figure 8 shows the XRD patterns of various a series samples of CXHP.

It can be seen from Figure 8 that the main diffraction peaks of all samples are basically consistent with the CXHP standard XRD card pattern. There is no sign of the presence of Ge element found from the XRD spectrum, which is probably because Ge ions replaced aluminum ions well into the octahedral site of CXHP, so other impurity phases did not appear obviously.

3.5. Attenuation Curve Analysis and Application Analysis. Figure 9 is the afterglow emission spectrum of CXHP samples with Cr^{3+} different doping components after being irradiated by an ultraviolet lamp with an average wavelength of 225 nm for 4.5 minutes and decreasing for 12 minutes.

It can be seen from Figure 9 that the sample has an afterglow ejection in the range of 645 nm to 740 nm, and the two emission peaks are located at 680 nm and 700 nm, respectively. The afterglow emission spectrum is basically consistent with the shape and emission peak position of the fluorescence spectrum, indicating that the emission center of the afterglow is Cr^{3+}, and the fluorescence emission and the afterglow emission also come from the Cr^{3+} ion 2E⟶4A2 feature span, and the R line at 680 nm is caused by the Cr^{3+} ion crossing that occupies the ideal polyhedron is generated, while the N2 line at 700 nm is formed by the Cr^{3+} ion 2E⟶4A2 energy level crossing with antipotential loopholes around it. The appearance of these two afterglow emission peaks once again proves that Cr^{3+} ions are in two different crystal field environments in the synthesized long-lasting luminescent material. CXHP samples without Cr^{3+} ions have very weak afterglow, which may be related to the intrinsic defects of the matrix, such as zinc vacancies, oxygen vacancies, and germanium vacancies. The above results indicate that Cr^{3+} ions not only act as luminescence centers but also play an important role in long afterglow luminescence. Figure 10 shows the afterglow decay curve of the series of samples CXHP.

It can be seen from Figure 10 that the sample is irradiated with a light with a center wavelength of 225 nm for 4.6 minutes before testing. The curve uses the afterglow decay time as the abscissa, and monitors the afterglow

Table 2: Main reagents and purity.

Name	Chemical	Purity	Manufacturer
Zinc oxide	ZnO	X.E+99.9%	National medicine group
Alumina	Al_2O_3	X.E+99.9%	National medicine group
Chromium oxide	Cr_2O_3	X.E+99.9%	National medicine group
Gallium oxide	Ca_2O_3	99.9999%	National medicine group
Oxide	GeO_2	99.9999%	National medicine group
Lithium carbonate	Li_2CO_3	99.9999%	National medicine group
Anhydrous ethanol	C_2H_5OH	Analyze pure	Chongqing Chuandong chemical

Table 3: The main equipment used by the experiment.

Name	Equipment model/specification	Manufacturer	Message accuracy
Electronic balance	TP-115	Sad Denver	93.6%
Box high-temperature sintered furnace	KSL-1600A	Hefei Crystal	94.2%
Powder tablet machine	LD-4X	Tianjin Expandorum Instrument	91.3%
Agate mortar	13 cm	Huanyu agate	90.5%
Planetary ball mill	AQN-2I	Nanjing science	96.5%
Ultrasound cleaning machine	FWXX-8090	Shanghai Song	96.6%
Dry box	WGK-7080X	Shanghai Dongyu	97.1%

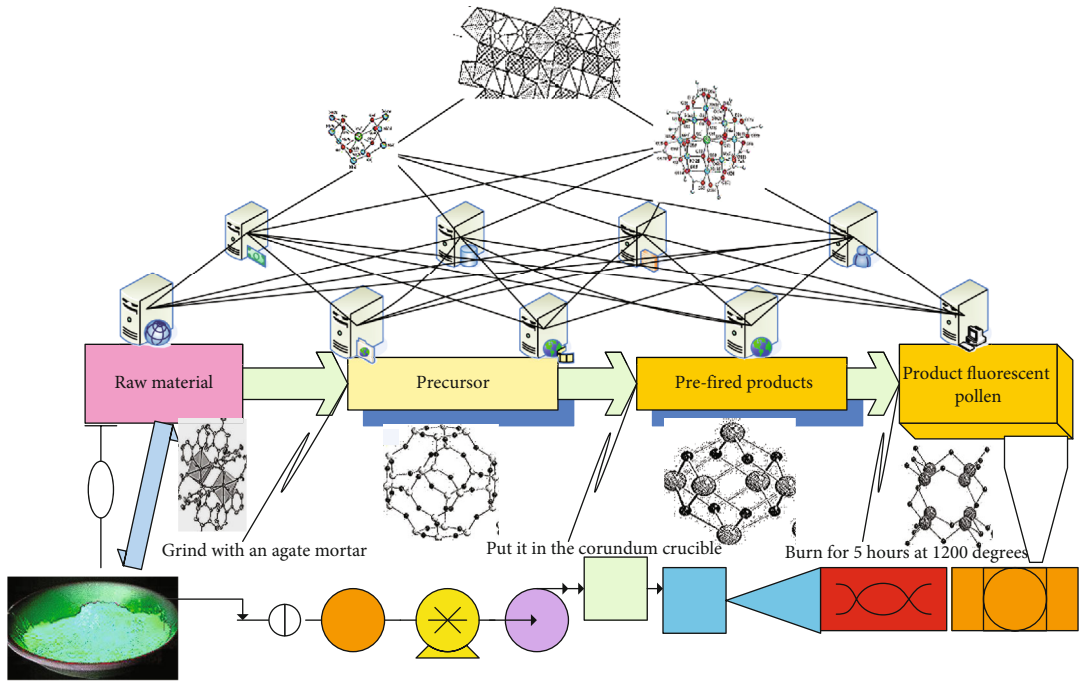

Figure 6: Flow diagram of high-temperature solid-state method.

emission at a wavelength of 680 nm and draws its luminous intensity as the ordinate, which can reflect the change state of the afterglow performance over time. There are two processes in the sample CXHP afterglow decay curve: fast decay process and slow decay process. The afterglow luminescence intensity of all samples decreased rapidly at the initial stage and then gradually became slow with the increase of time and lasted for a long period of time with corresponding intensity, indicating that there may be traps of different depths. We found that samples with different ion doping concentrations have different afterglow times and decay rates. As shown in the figure, when the concentration of doping Cr^{3+} increases,

Table 4: Synthetic conditions for ultrasmall object in different sizes.

Grain size	Types of alkali	The amount of alkali added	Reaction time	Temperature reflex
2.5	LIOH	3	115	298
3.3	LIOH	4.5	225	298
4.4	KOH	3	59	298
5.9	KOH	4.5	115	298
6.9	KOH	3.9	249	318

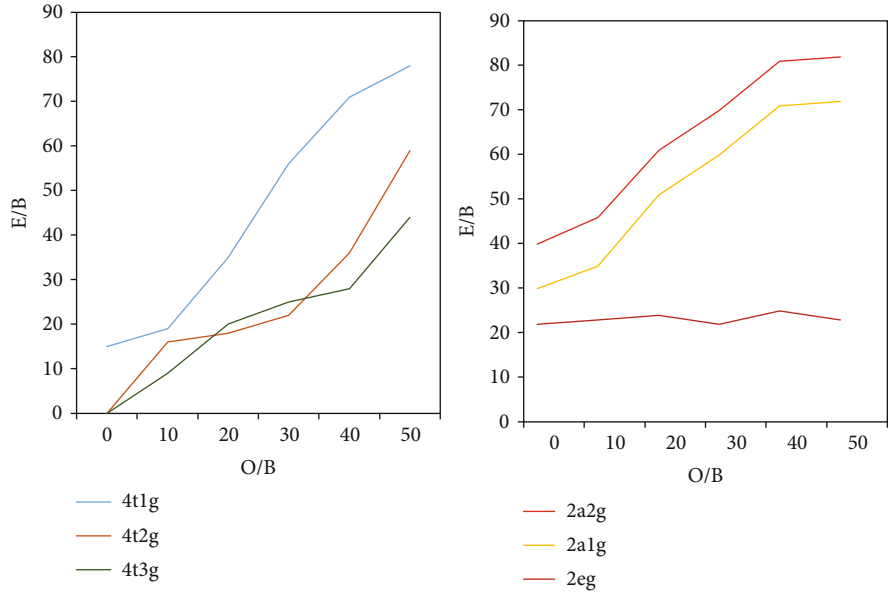

Figure 7: Energy level splitting in an octahedral crystal field.

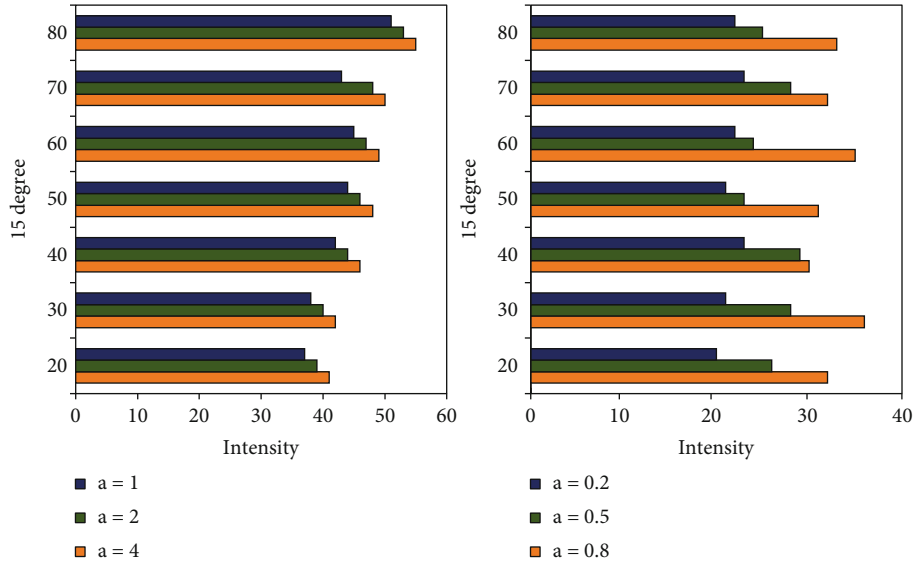

Figure 8: XRD patterns of various a series samples of CXHP.

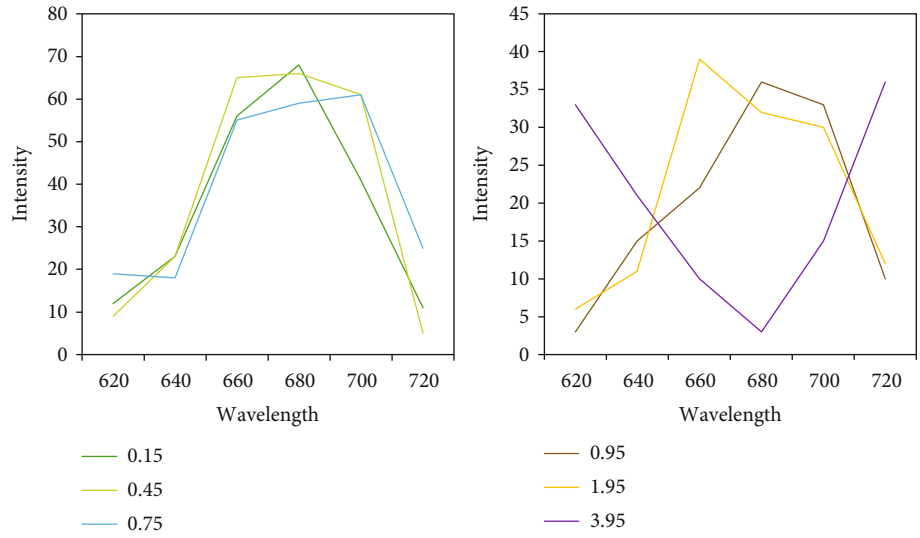

Figure 9: Afterglow spectra of CXHP multiple samples.

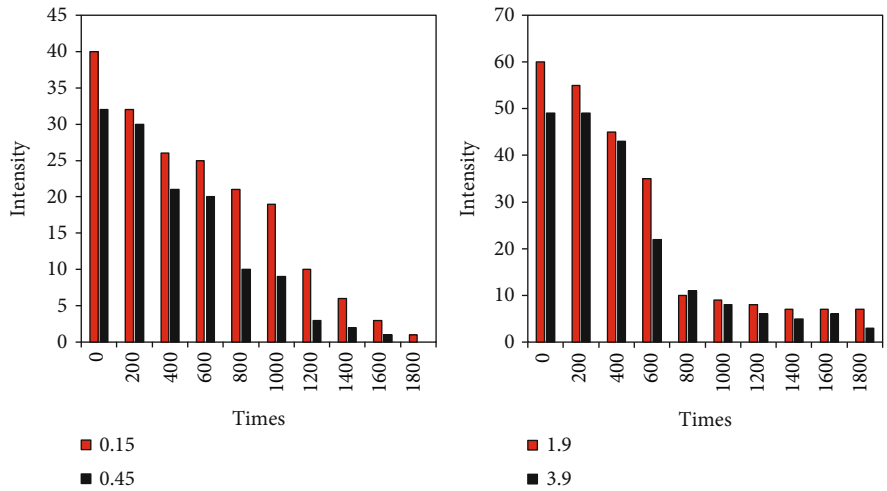

Figure 10: Afterglow decay curve of the sample.

Table 5: Dyeing experiment.

Experiment	Composite dosage	Dyeing effect	Accuracy	Experimental error
Experiment 1	0.6	Bad	99.6%	<0.5
Experiment 2	1.2	Just so so	99.6%	<0.1
Experiment 3	1.8	Good	99.3%	<0.05

the afterglow luminescence performance of the sample is gradually enhanced, reaching the highest point when the doping concentration is 1.9%, Unlike $a = 0.9\%$ fluorescence emission concentration quenching, CXHP afterglow concentration quenching may be due to the increase in the number of traps due to the increase of ion doping concentration. We found through experiments that the sample with a doping concentration of 1.9% has the best the afterglow performance; the afterglow time is more than 12 hours.

Then, the thoroughly optimized product was used in ethnic clothing. In order to achieve the color matching the purple luminous yarn used before, a series of dyeing experiments were carried out on the dye to achieve the best matching effect, as shown in Table 5. In the experiment, the amount of water used was 1500 ml, and the grams of composite material added for the three times were 0.6 g, 1.2 g, and 1.8 g, respectively. The hanging dyeing method was used during the experiment.

Through experiments, it can be obtained that when the composite material is 1.8 grams, and the visual effect is more similar to the hue, brightness, purity, and other aspects of the clothing. This way, when combined with composite materials for secondary design, a better visual effect will be achieved, so this composite material is used to dye the fabric. Although the types of colors are far inferior to traditional fabrics with diverse colors, delicate changes, and richness, it also has advantages that traditional fabrics do not have. Using the unique advantage of luminous effect, these two materials are recombined and designed. The color combination of luminous materials and ordinary textile materials in all aspects and multiple methods, in practice, find the best decorative combination form to be used in ethnic minority clothing, becoming the focus and highlight of color design, forming the visual center, and making clothing. The colors of the light form a visual effect similar to ordinary clothing in the light state, but in the dark state, it can also give play to the advantages of the material itself and show the color beauty of clothing in the dark.

4. Discussion

Upconversion luminescent materials have been tried to use in medical imaging, photodynamic therapy, temperature detection, infrared detection, and other fields and have achieved good results. However, during use, it will receive a certain amount of radiation from other high-energy particles such as X-rays and electron flow, and these radiations will bring about some changes in the characteristics of the material itself, and the upconversion luminescence characteristics of the material will also follow. The excellent performance of upconversion luminescent materials makes it applicable to temperature detection, environmental indicator warning, radiation intensity detection, etc. under conditions of outer space in the future. Luminescent materials in nanoaluminate are functional materials that can convert various forms of energy absorbed from the outside into nonequilibrium light radiation. Luminescent materials widely exist in people's life, and people have a perceptual understanding of this.

When designing, according to the style and characteristics of the clothing, we can make better use of the rebuilt luminous fabrics, which can innovate and change the design form of the traditional clothing partial shape, and the resulting changes can make the clothing produce refreshing sensory enjoyment. Through the design of the shape of the garment technology, the reorganization and shift design, and the sewing design, a solid foundation has been laid for the sewing and inlaying of pieces of reconstituted fabrics, which can achieve an unexpected and reasonable form effect, so that remanufactured fabrics play a finishing touch to the local shape of clothing. Whether it is the hand crocheting of the fabric for decorative effects in the secondary regeneration, or the basting before the perfect stitching of the reconstituted fabric and the ordinary fabric, it shows the demand of the reconstituted fabric for the garment craftsmanship. The material innovation of clothing fabrics and the innovation of fabric remanufacturing techniques can both cause changes in the clothing production process and can add new design techniques and a steady stream of artistic charm to the design of ethnic minority clothing.

5. Conclusions

This thesis mainly focuses on the design and application of luminous materials, namely luminous yarns and luminous paints, in the design and application of ethnic minority clothing. In order to achieve this goal, this article uses a variety of scientific methods mainly in the fields of material preparation, clothing design, etc., and analyzes luminescent composite materials. Finally, a luminescent composite material that can act in this field was designed. Based on the preparation of the previous material, the afterglow attenuation performance of this composite material was studied. Before the test, the sample was irradiated with an ultraviolet lamp with a center wavelength of 225 nm for 4.6 minutes. The curve uses the afterglow decay time as the abscissa and monitors the afterglow emission at a wavelength of 680 nm and draws its luminous intensity as the ordinate, which can reflect the change of the afterglow performance over time. When the concentration of Cr ion is increased, the afterglow luminescence intensity of the sample is gradually enhanced, reaching the maximum value when the doping concentration is 1.9%, and then weakening due to the quenching effect of the afterglow concentration, which is consistent with the changing trend of the afterglow spectrum. We found through experiments that the sample with a doping concentration of 1.9% has the best afterglow performance, and the afterglow time exceeds 12 hours. At the same time, when the number of grams of composite materials is 1.8, the optimization design will get more practical and exquisite products. The shortcomings of this paper are as follows: firstly, in the process of the combination of composite luminescent materials and traditional technology, only a few representative practical forms are selected. Secondly, at this stage, the research on the development and application of follow-up products of luminous materials, especially clothing products, mostly stays in the surface stage. In the application, it mainly shows the functional design of luminous materials. The decorative and aesthetic characteristics of this material need to be further excavated. Therefore, in further research, we should not only focus on the excellence of luminous performance but also integrate with a variety of traditional processes to make the appearance of clothing more beautiful, but also more in line with the characteristics of ethnic minority clothing.

Data Availability

The data underlying the results presented in the study are available within the manuscript.

Conflicts of Interest

The authors declare that they have no conflicts of interest.

Acknowledgments

This work was supported by the 2020 Hunan Social Science Project "Research on the Development path of Weaving and embroidery Entrepreneurship Workshop for ethnic minorities in Xiangxi under the Mode of "nonlegacy + Poverty Alleviation"" (No.: 20YBA211) and the 2019 Hunan Provincial Department of Education Project: "Exploration of Innovation and Entrepreneurship of ethnic Minority handweaving and embroidery artists in Western Hunan from the Perspective of Poverty Alleviation through Education" (No.: 19C1479).

References

[1] J. Kaewkhao, N. Wantana, S. Kaewjaeng, S. Kothan, and H. J. Kim, "Luminescence characteristics of Dy^{3+} doped Gd_2O_3-CaO- SiO_2-B_2O_3 scintillating glasses," *Journal of Rare Earths*, vol. 34, no. 6, pp. 583–589, 2016.

[2] A. M. Hernández, M. Alfaro, A. B. Villatoro, C. Falcony, T. R. Montalvo, and J. Z. Medina, "Luminescence characteristics of $LaAlO_3$:Eu^{3+} obtained by modified Pechini's method," *Open Journal of Synthesis Theory and Applications*, vol. 6, no. 1, pp. 1–12, 2017.

[3] V. I. Oleshko, V. F. Tarasenko, D. V. Beloplotov, and S. S. Vil'chinskaya, "Spectral and kinetic characteristics of the luminescence of Ga2O3 crystals excited by nano- and subnanosecond electron beams," *Optics and Spectroscopy*, vol. 125, no. 5, pp. 627–631, 2018.

[4] O. N. Bezkrovnaya, V. V. Maslov, I. M. Pritula et al., "Spectral-luminescence characteristics of laser dyes in a calcined xerogel," *Journal of Applied Spectroscopy*, vol. 84, no. 1, pp. 31–34, 2017.

[5] K. Kyselova and O. Shandrenko, "The ways to find harmony in modern clothing design projects," *Demiurge Ideas Technologies Perspectives of Design*, vol. 4, no. 1, pp. 59–69, 2021.

[6] K. D. Krause, F. Kapadia, D. C. Ompad, P. A. D'Avanzo, D. T. Duncan, and P. N. Halkitis, "Early life psychosocial stressors and housing instability among young sexual minority men: the P18 cohort study," *Journal of Urban Health-bulletin of the New York Academy of Medicine*, vol. 93, no. 3, pp. 511–525, 2016.

[7] A. Ghosh, A. Kumar, A. Roy et al., "Ultrathin lithium aluminate nanoflake-inlaid sulfur as a cathode material for lithium –sulfur batteries with high areal capacity," *ACS Applied Energy Materials*, vol. 3, no. 6, pp. 5637–5645, 2020.

[8] P. Zhao, H. Wang, S. Wang, P. du, L. Lu, and X. Cheng, "Assessment of nano-TiO2 enhanced performance for photocatalytic polymer-sulphoaluminate cement composite coating," *Journal of Inorganic and Organometallic Polymers and Materials*, vol. 28, no. 6, pp. 2439–2446, 2018.

[9] A. Ebrahimzade, M. Mojtahedi, and R. S. Rahbar, "Study on characteristics and afterglow properties of luminous polypropylene/ rare earth strontium aluminate fiber," *Journal of Materials Science Materials in Electronics*, vol. 28, no. 11, pp. 8167–8176, 2017.

[10] Y. Jin, X. Long, Y. Zhu, and M. Ge, "Optical performance study of $Sr_2ZnSi_2O_7$:Eu^{2+},Dy^{3+}, $SrAl_2O_4$:Eu^{2+},Dy^{3+} and Y_2O_2S:Eu^{3+}, Mg^{2+},Ti^{4+} ternary luminous fiber," *Journal of Rare Earths*, vol. 34, no. 12, pp. 1206–1212, 2016.

[11] G. I. Akmehmet, S. Šturm, M. Komelj et al., "Origin of long afterglow in strontium aluminate phosphors: atomic scale imaging of rare earth dopant clustering," *Ceramics International*, vol. 45, no. 16, pp. 20073–20077, 2019.

[12] H. J. Jeong, D.-W. Jeon, J.-H. Kim et al., "Mixed alkali effect on the luminescence characteristics of color conversion glasses," *Journal of Ceramic Processing Research. (Text in English)*, vol. 17, no. 7, pp. 694–698, 2016.

[13] Y. Zhang and X. Wang, "A comparative study of Heilongjiang minority costumes and customs (taking Oroqen and Manchu as examples)," *Historical and Social-educational Ideas*, vol. 13, no. 1, pp. 79–92, 2021.

[14] J. Webber, K. Moran, C. French, F. Fozard, and O. Pearless, "Fatal coastal drowning incidents: a 10-year review of body recovery times in New Zealand," *Forensic Science International*, vol. 317, no. 12, pp. 110573–110577, 2020.

[15] M. K. Chung, "Analysis of character education elements in the field of clothing & textiles of practical arts education – focusing on character education promotion act," *Journal of Korean Practical Arts Education*, vol. 23, no. 4, pp. 15–31, 2017.

[16] D. Damianos, G. Vitrant, A. Kaminski-Cachopo et al., "Field-effect passivation of Si by ALD-Al_2O_3: second harmonic generation monitoring and simulation," *Journal of Applied Physics*, vol. 124, no. 12, p. 125309, 2018.

[17] Z. B. Ramazanova, "Traditional men's clothing of the peoples of Nagorny Dagestan: ecological functions," *History Archeology and Ethnography of the Caucasus*, vol. 14, no. 4, pp. 158–165, 2018.

[18] B. Gao, X. Ning, and P. Xing, "Shock wave induced nanocrystallization during the high current pulsed electron beam process and its effect on mechanical properties," *Materials Letters*, vol. 237, no. 15, pp. 180–184, 2019.

[19] X. Guo, H. Shi, C. Wei, and X. D. Chen, "Research on thermal property and temperature rating prediction of Mongolian robe ensembles," *International Journal of Clothing Science and Technology*, vol. 30, no. 6, pp. 747–756, 2018.

[20] A. A. Pesetskaya, "Clothing as a part of the Mari wedding gift exchange (the late 19th and early 20th centuries)," *Yearbook of Finno-Ugric Studies*, vol. 13, no. 2, pp. 312–324, 2019.

[21] S. Hong and K. H. Choi, "Characteristics of luminescence signals according to the depositional environment," *Journal of the Korean Geomorphological Association*, vol. 28, no. 2, pp. 59–70, 2021.

[22] L. E. Muresan, E. J. Popovici, I. Perhaita, E. Indrea, J. Oro, and N. Casan Pastor, "Rare earth activated yttrium aluminate phosphors with modulated luminescence," *Luminescence*, vol. 31, no. 4, pp. 929–936, 2016.

[23] Z. Liu, S. Li, Y. Huang et al., "Composite ceramic with high saturation input powder in solid-state laser lighting: microstructure, properties, and luminous emittances," *Ceramic Materials*, vol. 44, no. 16, pp. 20232–20238, 2018.

[24] Y. Tang, Z. Chen, W. Feng, Y. Nong, C. Li, and J. Chen, "Combined effects of nano-silica and silica fume on the mechanical behavior of recycled aggregate concrete," *Nanotechnology Reviews*, vol. 10, no. 1, pp. 819–838, 2021.

[25] S. Chen, X. Hou, X. Li, and M. Ge, "Preparation and characterization of persistent luminescence of regenerated cellulose fiber," *Journal of Materials Science: Materials in Electronics*, vol. 28, no. 1, pp. 1015–1021, 2017.